Structural Engineering and Mechanics, Vol. 13, No. 4 (2002) 411-428
DOI: http://dx.doi.org/10.12989/sem.2002.13.4.411

Thermomechanical buckling of rectangular, shear-deformable, composite laminated plates

Y. S. Ge†, W. X. Yuan‡ and D. J. Dawe‡†

Department of Civil Engineering, The University of Birmingham, Edgbaston, Birmingham B15 2TT, UK

Abstract. The B-spline finite strip method is developed for the prediction of the buckling of rectangular composite laminated plates under the combined action of applied uniaxial mechanical stress and increasing temperature. The analysis is conducted in two stages, namely an in-plane stress analysis in the pre-buckling stage to determine the pre-buckling stresses, followed by a buckling analysis using these determined stresses. The buckling analysis is based on the use of first-order shear deformation plate theory. The permitted lay-up of the laminates is quite general, within the constraint that the plate remains flat prior to buckling, and a wide range of boundary conditions can be accommodated. A number of applications is described and comparison of the results generated using the finite strip method is made with the results of previous studies.

Key words: buckling; thermomechanical; plates; laminates; shear deformation; finite strip.

1. Introduction

A considerable body of literature exists on the buckling of rectangular composite laminated plates subjected to mechanical loads and a quite recent book, edited by Turvey and Marshall (1995), contains much information on this subject area. A lesser body of information exists on the buckling of such plates under thermal loading but within the aforementioned book Tauchert (1995) has presented a review of work on thermal (and hygrothermal) buckling, and a later study by Dawe and Ge (2000) includes reference to numerous pertinent works. The problem of buckling under the combined action of thermal and mechanical loading has been considered by relatively few investigators but is of importance and is the focus of attention in the present paper.

In dealing with the combined problem the critical buckling temperatures for initially-stressed, thick, simply supported plates were determined using the Galerkin method by Chen *et al.* (1982), for isotropic plates, and by Yang and Shieh (1988) for anti-symmetric cross-ply laminates. A study of the buckling of composite laminated plates subjected to combined thermal and axial mechanical loadings was presented by Noor and Peters (1992) using a mixed finite element approach in the context of Reissner-Mindlin first-order shear deformation plate theory (referred to simply as SDPT here). This approach was extended by Noor and Peters (1993) to embrace postbuckling behaviour, incorporating a multi-parameter reduction method (as in their earlier work) in determining stability

† Research Student : now Principal Structural Analyst, SERCK Aviation
‡ Research Student : now Research Fellow, Department of Chemical Engineering
‡† Professor of Structural Mechanics

boundaries and postbuckling responses. Sai Ram and Sinha (1992) investigated the effects of temperature and moisture on the stability of composite laminated plates subjected to in-plane loads. They used a finite element method (FEM) in the context of SDPT, incorporating reduced lamina material properties at elevated temperatures, and considered symmetric and anti-symmetric laminates with simply-supported and clamped boundaries.

The B-spline finite strip method (B-s FSM) in the context of SDPT is developed here for the analysis of the thermomechanical buckling of rectangular laminates. The B-s FSM was introduced by Cheung and Fan (1983) in studying the static behaviour of box girder bridges in the context of classical plate theory (CPT). More recently, it has been developed in the context of both CPT and SDPT for a range of types of application which include mechanical buckling of both single plates and complicated plate structures (Dawe and Wang 1994, 1995, Dawe 1995, Wang and Dawe 1997) and thermal buckling of single plates (Dawe and Ge 2000). The present report extends this successful analysis approach, in the context of SDPT, to the study of thermomechanical buckling behaviour and presents description of a number of applications for which earlier, comparative results are available.

2. Finite strip method

2.1 Preamble

The flat rectangular plate under consideration, of length A (in the x-direction), width B (in the y-

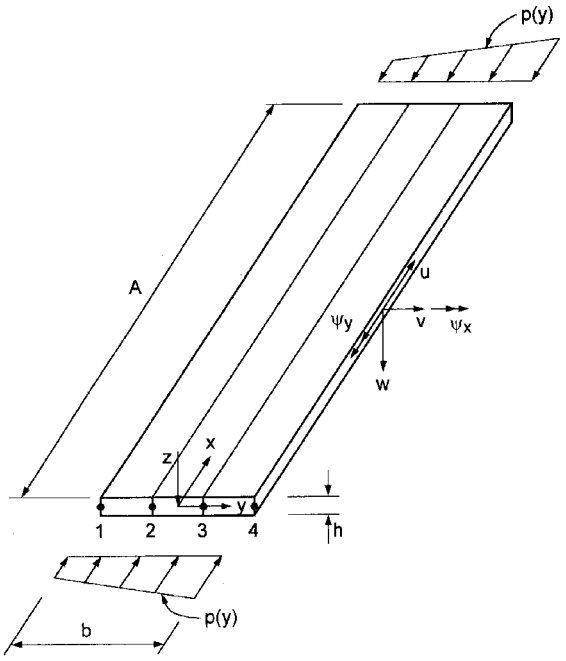

Fig. 1 A finite strip

direction) and thickness h (in the z-direction) is modelled with a number of finite strips of the type shown in Fig. 1, of width $b \leq B$. In general the plate may be a laminate formed of N layers of unidirectional fibre-reinforced composite material. From a stress-free state the plate may be subjected to a temperature rise $T(x, y)$ which does not vary through the thickness but may be non -uniform in the plane of the plate, and/or to mechanical loading $p(y)$ per unit width at its ends $x = 0$, A as indicated for a strip in Fig. 1.

It is assumed that under the action of increasing temperature and/or mechanical loading the plate remains flat as in-plane stresses develop progressively, until these stresses reach a critical level at which out-of-plane, bifurcational buckling occurs. This assumption has implications for the range of laminate lay-ups that can be accommodated. It naturally includes all symmetrically laminated, or balanced, plates but it does not necessarily exclude all anti-symmetric unbalanced plates. Pertinent to this, Leissa (1986) and Qatu and Leissa (1993) have shown that specific unbalanced laminates with particular boundary conditions will remain flat when acted upon by particular distributions of in-plane stress. This statement includes anti-symmetric angle-ply laminates with simply supported or clamped edges when subjected to uniform or linearly-varying in-plane direct stresses. It also includes anti-symmetric cross-ply laminates with clamped edges when subjected to uniform in-plane direct stresses. Hence there is justification for including some in-plane to out-of-plane coupling terms in the laminate constitutive equation at the onset of buckling (as will be done below).

In line with the assumption of bifurcational buckling there is a need to determine, in the first stage, the pre-buckling distribution of membrane stresses. Such determination may be trivial in situations where stresses are clearly uniform or may be complicated in other situations where it is necessary to conduct a plane stress, finite strip analysis to determine the non-uniform, pre-buckling, in-plane stress distribution. In either situation the pre-buckling stresses are taken forward to the second stage of the analysis where they enter into the plate geometric stiffness matrix in an eigenvalue buckling calculation. The two distinct stages of calculation are described separately in what follows but it is noted that the same number and width of strips is used in each stage.

2.2 Pre-buckling plane stress analysis

The displacement field of a finite strip in the pre-buckled state is assumed to be of the form

$$\begin{Bmatrix} u \\ v \end{Bmatrix} = \sum_{i=1}^{n+1} \begin{bmatrix} N_i & 0 \\ 0 & N_i \end{bmatrix} \begin{bmatrix} \bar{\boldsymbol{\Phi}}_k & \mathbf{0} \\ \mathbf{0} & \bar{\boldsymbol{\Phi}}_k \end{bmatrix} \begin{Bmatrix} \boldsymbol{d}^u \\ \boldsymbol{d}^v \end{Bmatrix}_i \quad \text{or} \quad \boldsymbol{\delta} = \sum_{i=1}^{n+1} \boldsymbol{N}_i \boldsymbol{S} \boldsymbol{d}_i. \tag{1}$$

Here the $N_i = N_i(y)$ are standard Lagrangian shape functions of degree n running across the strip which has $(n + 1)$ reference lines at which degrees of freedom are located. The finite strip shown in Fig. 1 corresponds to $n = 3$ (i.e., a cubic strip) with four (numbered) reference lines. The $\bar{\boldsymbol{\Phi}}_k = \bar{\boldsymbol{\Phi}}_k(x)$ are modified B-spline function bases of degree k running along the strip and $\boldsymbol{d}^u$ and $\boldsymbol{d}^v$ are column matrices of degrees of freedom associated with u and v, respectively. The spline knots are equi-spaced along the strip length, with q spline sections and $q + 1$ knots in the length A, as shown in Fig. 2a, plus other knots outside each end of this length which are required for the purposes of completing the definition of a function and prescribing end conditions. The individual local spline functions $\bar{\boldsymbol{\Phi}}_k(x)$ of polynomial degree k (for $k = 1$ to 5) are defined algebraically elsewhere (Dawe and Wang 1992) : here Fig. 2b shows a local cubic B_3-spline function ($k = 3$)

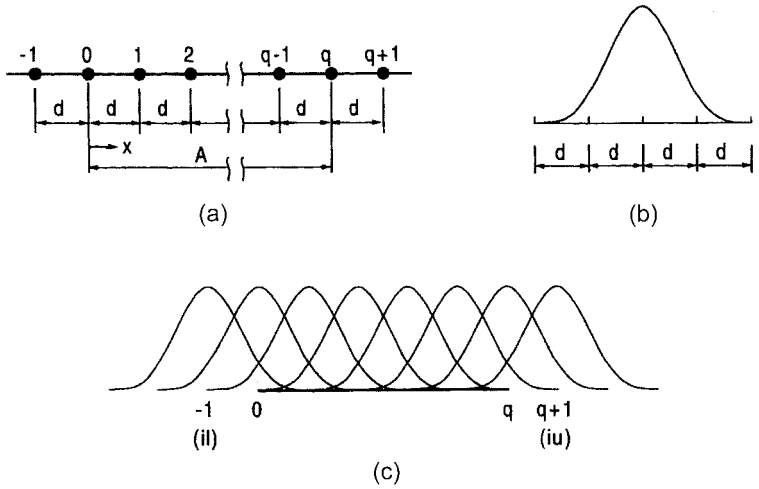

Fig. 2 Spline representation: (a) spline sections and knots; (b) local cubic spline functions; and (c) a combination of cubic spline functions.

whilst Fig. 2c shows the juxtaposition of such local functions to form a complete function. The modified B-spline function basis $\overline{\mathbf{\Phi}}_k(x)$ incorporates revisions to the original function basis, so as to facilitate the specification of end conditions. Such revisions can be made in more than one way but here they follow the procedures of Dawe and Wang (1992). For $k = 3$, for instance, and in representing u (with similar considerations applying to the representation of v), the $\overline{\mathbf{\Phi}}_k(x)$ corresponds to a definition of the column matrix $\boldsymbol{d}_i^u$ of degrees of freedom associated with the u-displacement, as

$$\boldsymbol{d}_i^u = \{u_o \; u_o' \;\; \alpha_1 \; \alpha_2 \ldots \alpha_{q-1} \; u_q \; u_q' \}_i . \tag{2}$$

Here α_1 to α_{q-1} are generalised coefficients, u_o and u_o' are values of u and du/dx at spline knot 0, and u_q and u_q' are similarly defined at knot q.

The linear stress-strain relationships of an individual, orthotropic layer, related to the x, y axes, have the form

$$\begin{Bmatrix} \sigma_x \\ \sigma_y \\ \tau_{xy} \end{Bmatrix} = \begin{bmatrix} Q_{11} & Q_{12} & Q_{16} \\ Q_{12} & Q_{22} & Q_{26} \\ Q_{16} & Q_{26} & Q_{66} \end{bmatrix} \begin{Bmatrix} \varepsilon_x - \alpha_x T \\ \varepsilon_y - \alpha_y T \\ \gamma_{xy} - 2\alpha_{xy} T \end{Bmatrix} \tag{3}$$

where α_x, α_y and α_{xy} are thermal expansion coefficients, $T = T(x, y)$ is the temperature rise, σ_x, σ_y and τ_{xy} are the stresses, the Q_{rs} $(r, s = 1, 2, 6)$ are transformed layer stiffness coefficients, and ε_x, ε_y and γ_{xy} are the linear strains which are defined as

$$\varepsilon_x = \frac{\partial u}{\partial x}, \quad \varepsilon_y = \frac{\partial v}{\partial y}, \quad \gamma_{xy} = \frac{\partial u}{\partial y} + \frac{\partial v}{\partial x} . \tag{4}$$

The corresponding constitutive equations for the laminate plane stress behaviour are

$$\begin{Bmatrix} N_x \\ N_y \\ N_{xy} \end{Bmatrix} = \int_{-h/2}^{h/2} \begin{Bmatrix} \sigma_x \\ \sigma_y \\ \tau_{xy} \end{Bmatrix} dz = \begin{bmatrix} A_{11} & A_{12} & A_{16} \\ A_{12} & A_{22} & A_{26} \\ A_{16} & A_{26} & A_{66} \end{bmatrix} \left(\begin{Bmatrix} \varepsilon_x \\ \varepsilon_y \\ \gamma_{xy} \end{Bmatrix} - T \begin{Bmatrix} \alpha_x \\ \alpha_y \\ 2\alpha_{xy} \end{Bmatrix} \right)$$

or

$$\boldsymbol{F} = \boldsymbol{L}(\boldsymbol{e} - \boldsymbol{e}_t). \tag{5}$$

Here $\boldsymbol{e}$ and $\boldsymbol{e}_t$ are the column matrices of elastic and thermal strains, respectively; N_x N_y and N_{xy} in $\boldsymbol{F}$ are the membrane direct and shearing forces per unit length; and the stiffness coefficients appearing in $\boldsymbol{L}$ are defined by

$$A_{rs} = \int_{-h/2}^{h/2} Q_{rs} dz, \qquad r, s = 1, 2, 6. \tag{6}$$

During the deformation process the change in total potential energy of a finite strip is

$$\Pi = U + V \tag{7}$$

where U is the strain energy and V is the potential energy of the applied loading at the two ends $x = 0, A$.

The strain energy can be expressed as (Dawe and Ge 2000)

$$U = U_1 - 2U_2 + U_3 \tag{8}$$

where

$$U_1 = \frac{1}{2} \int_{-b/2}^{b/2} \int_o^A \boldsymbol{e}^T \boldsymbol{L} \boldsymbol{e} dx dy, \tag{9}$$

$$U_2 = \frac{1}{2} \int_{-b/2}^{b/2} \int_o^A \boldsymbol{e}^T \boldsymbol{L} \boldsymbol{e}_t dx dy, \tag{10}$$

$$U_3 = \frac{1}{2} \int_{-b/2}^{b/2} \int_o^A \boldsymbol{e}_t^T \boldsymbol{L} \boldsymbol{e}_t dx dy. \tag{11}$$

Using Eqs. (1) and (3) the elastic strains $\boldsymbol{e}$ can be expressed as

$$\boldsymbol{e} = \sum_{i=1}^{n+1} \begin{bmatrix} N_i \overline{\boldsymbol{\Phi}}_k' & \boldsymbol{0} \\ \boldsymbol{0} & N_i' \overline{\boldsymbol{\Phi}}_k \\ N_i' \overline{\boldsymbol{\Phi}}_k & N_i \overline{\boldsymbol{\Phi}}_k' \end{bmatrix} \begin{Bmatrix} \boldsymbol{d}^u \\ \boldsymbol{d}^v \end{Bmatrix}_i = \sum_{i=1}^{n+1} \boldsymbol{B}_i \boldsymbol{d}_i \tag{12}$$

where the prime ( )' denotes differentiation with respect to x for $\overline{\boldsymbol{\Phi}}_k(x)$ and with respect to y for $N_i(y)$. It then follows (Dawe and Ge 2000) that U_1 can be written in the form

$$U_1 = \frac{1}{2} \boldsymbol{d}^T \boldsymbol{k} \boldsymbol{d} \tag{13}$$

with typical submatrix $\boldsymbol{k}_{ij}$ ($i, j = 1, 2 \cdots n + 1$) of the strip stiffness matrix $\boldsymbol{k}$ defined as

$$\boldsymbol{k}_{ij} = \int_{-b/2}^{b/2}\int_{o}^{A} \boldsymbol{B}_i^T \boldsymbol{L} \boldsymbol{B}_j dxdy \tag{14}$$

and where $\boldsymbol{d}$ is the column matrix of all strip degrees of freedom. It also follows that U_2 can be written as

$$U_2 = \frac{1}{2}\boldsymbol{d}^T \boldsymbol{f}_t \tag{15}$$

with the typical submatrix $\boldsymbol{f}_{ti}$ of the thermal loading column matrix $\boldsymbol{f}_t$ defined as

$$\boldsymbol{f}_{ti} = \int_{-b/2}^{b/2}\int_{o}^{A} \boldsymbol{B}_i^T \boldsymbol{L} \boldsymbol{e}_t dxdy. \tag{16}$$

In $\boldsymbol{e}_t$ (see Eq. 5) the variation allowed for T over the strip surface is that T can vary across the strip (with y) as a polynominal function of degree three, using Lagrangian interpolation, and can vary linearly (with x) along the strip.

The third part, U_3, of the strain energy need not be considered in any further detail since it is not a function of the strip freedoms $\boldsymbol{d}$ and hence will play no part when the total potential energy is minimised.

The potential energy of the applied mechanical loading is

$$V = -\int_{-b/2}^{b/2} p(u)_{x=0} dy + \int_{-b/2}^{b/2} p(u)_{x=A} dy. \tag{17}$$

Clearly the integrations are made only over the ends of the finite strip and the effective expression for u in each of the integrations is the particular reduced form of the general expression for u (given in Eq. 1) that applies at the end. Thus

$$V = -\int_{-b/2}^{b/2} \left(p \sum_{i=1}^{n+1} N_i (\overline{\boldsymbol{\Phi}}_k \boldsymbol{d}_i^u)_{x=0} \right) dy + \int_{-b/2}^{b/2} \left(p \sum_{i=1}^{n+1} N_i (\overline{\boldsymbol{\Phi}}_k \boldsymbol{d}_i^u)_{x=A} \right) dy \tag{18}$$

which can be written in the form

$$V = -\boldsymbol{d}^T \boldsymbol{f}_m \tag{19}$$

where the typical submatrix $\boldsymbol{f}_{mi}$ of the mechanical loading column matrix $\boldsymbol{f}_m$ is defined as a column matrix of zeros except for entries of

$$\int_{-b/2}^{b/2} p N_i (\overline{\boldsymbol{\Phi}}_k)_{x=0} dy \quad \text{and} \quad -\int_{-b/2}^{b/2} p N_i (\overline{\boldsymbol{\Phi}}_k)_{x=A} dy$$

in the first and last-but-one positions (i.e., in positions corresponding to u_i at $x = 0$ and $x = A$, respectively).

The total potential energy of a finite strip now becomes, using Eqs. (6), (7), (12), (14) and (18),

$$\Pi = \frac{1}{2}\boldsymbol{d}^T \boldsymbol{k} \boldsymbol{d} - \boldsymbol{d}^T \boldsymbol{f}_t - \boldsymbol{d}^T \boldsymbol{f}_m + U_3. \tag{20}$$

The integrations involved in evaluating $\boldsymbol{k}$, $\boldsymbol{f}_t$ and $\boldsymbol{f}_m$ are performed analytically in the y-direction and numerically in the x-direction through Gaussian integration with four points per spline section.

For the complete plate an expression of the same form applies, but written in terms of the plate stiffness matrix $\boldsymbol{K}$, degrees of freedom $\boldsymbol{D}$, thermal load column matrix $\boldsymbol{F}_t$ and mechanical load column matrix $\boldsymbol{F}_m$ rather than their lower-case equivalents in Eq. (20). The plate matrices are obtained by appropriate super-imposition of the strip matrices in the standard direct stiffness procedure. If it is assumed that $\boldsymbol{K}$, $\boldsymbol{D}$, $\boldsymbol{F}_t$ and $\boldsymbol{F}_m$ denote plate matrices after the prescribed kinematic boundary conditions have been applied, then the minimisation of the plate total potential energy gives the set of equations

$$\boldsymbol{K}\,\boldsymbol{D} = \boldsymbol{F}_t + \boldsymbol{F}_m. \tag{21}$$

Solution of these equations for the degrees of freedom $\boldsymbol{D}$ is obtained using Gaussian elimination. When $\boldsymbol{D}$ is known, and hence $\boldsymbol{d}$ for each strip, the forces per unit length N_x, N_y and N_{xy} can be determined using Eqs. (4) and (5). The corresponding pre-buckling stresses are denoted as $\sigma_x^{\,o}$, $\sigma_y^{\,o}$ and $\tau_{xy}^{\,o}$, respectively, and are obtained from the forces per unit length by dividing by the plate thickness h.

2.3 Buckling analysis

In the second-stage analysis the flat laminated plate is subjected to the pre-buckling membrane stresses whose distributions are available from the first-stage analysis described above. Now ordinarily the situation will not be that the temperature and the end thrust increase directly proportionally in some known fashion until buckling occurs. Rather, two practical situations are considered here. The first situation is that the temperature increases a known amount (which is less than that which will cause buckling on its own) and it is required to find the critical value of end thrust which will then cause buckling. The second situation is that the end thrust is known (at a level not leading to buckling on its own) and it is required to find the critical value of temperature rise which will then cause buckling. Hence, in the pre-buckling stage what is required is two separate solutions for Eq. (21) and the subsequent determination of stresses : one for $\boldsymbol{F}_t = \boldsymbol{0}$ and a specified magnitude (unity say) of end thrust, and the other for $\boldsymbol{F}_m = \boldsymbol{0}$ and a specified magnitude (again unity say) of temperature increase. Then the total pre-buckling stresses moving forward to the buckling analysis will comprise an initial specified (in distribution and magnitude), or “dead”, stress system plus an imposed, or “live”, system whose distribution is known but whose magnitude which will cause buckling is not. Thus we will have a pre-buckling stress system of the form

$$\boldsymbol{\sigma}^o = \boldsymbol{\sigma}_D^o + \lambda\boldsymbol{\sigma}_L^o \tag{22}$$

where subscripts D and L denote the dead and live systems, respectively, λ is a load factor and $\boldsymbol{\sigma}^o = \{\sigma_x^o\ \sigma_y^o\ \tau_{xy}^o\}$ etc.

The aim now in the second stage of the analysis is to determine the critical value of λ that causes out-of-plane buckling. The buckling analysis is conducted in the context of Reissner-Mindlin first-order shear deformation plate theory. In this stage the displacements (and quantities derived from them) that occur are to be regarded as perturbation displacements, i.e., are to be regarded now as the changes of displacements that occur at the moment of buckling. In fact u and v are such changes but the displacements relating to out-of-plane deformation, i.e., the deflection w and the rotations of

the plate normal, ψ_x and ψ_y (see Fig. 1), are total displacements since there are no out-of-plane displacements in the first analysis stage.

The perturbation displacement field for the buckling problem is assumed to be

$$\begin{Bmatrix} u \\ v \\ w \\ \psi_y \\ \psi_x \end{Bmatrix} = \sum_{i=1}^{n+1} \begin{bmatrix} N_i & 0 & 0 & 0 & 0 \\ 0 & N_i & 0 & 0 & 0 \\ 0 & 0 & N_i & 0 & 0 \\ 0 & 0 & 0 & N_i & 0 \\ 0 & 0 & 0 & 0 & N_i \end{bmatrix} \begin{bmatrix} \bar{\boldsymbol{\Phi}}_k & \mathbf{0} & \mathbf{0} & \mathbf{0} & \mathbf{0} \\ \mathbf{0} & \bar{\boldsymbol{\Phi}}_k & \mathbf{0} & \mathbf{0} & \mathbf{0} \\ \mathbf{0} & \mathbf{0} & \bar{\boldsymbol{\Phi}}_k & \mathbf{0} & \mathbf{0} \\ \mathbf{0} & \mathbf{0} & \mathbf{0} & \bar{\boldsymbol{\Phi}}_k & \mathbf{0} \\ \mathbf{0} & \mathbf{0} & \mathbf{0} & \mathbf{0} & \bar{\boldsymbol{\Phi}}_{k-1} \end{bmatrix} \begin{Bmatrix} \boldsymbol{d}^u \\ \boldsymbol{d}^v \\ \boldsymbol{d}^w \\ \boldsymbol{d}^{\psi_y} \\ \boldsymbol{d}^{\psi_x} \end{Bmatrix}_i$$

which again is of the form

$$\boldsymbol{\delta} = \sum_{i=1}^{n+1} \boldsymbol{N}_i \boldsymbol{S} \boldsymbol{d}_i \tag{23}$$

where the definitions of the various quantities is along similar lines to that following Eq. (1). Here again the N_i are Lagrangian shape functions in the y-direction. The $\bar{\boldsymbol{\Phi}}_k$ and $\bar{\boldsymbol{\Phi}}_{k-1}$ are modified B-spline function bases of degrees k and $k-1$, respectively, in the x-direction : a lower degree of spline representation is used for the longitudinal variation of ψ_x than for the other four displacement quantities so as to avoid any shear-locking problem that may otherwise occur while analysing thin plates (Dawe and Wang 1992, 1994, 1995, Dawe 1995, Wang and Dawe 1997).

The in-plane (perturbation) stress-strain relationships of the individual layer, related to the laminate axes, are as in Eq. (3) but without the thermal contributions. These relationships are now augmented by the relationships

$$\begin{Bmatrix} \tau_{yz} \\ \tau_{zx} \end{Bmatrix} = \begin{bmatrix} Q_{44} & Q_{45} \\ Q_{45} & Q_{55} \end{bmatrix} \begin{Bmatrix} \gamma_{yz} \\ \gamma_{zx} \end{Bmatrix} \tag{24}$$

between the through-thickness shear stresses τ_{yz} and τ_{zx} and the corresponding shear strains γ_{yz} and γ_{zx}, where the Q_{rs} (r, $s = 4$, 5) are transformed stiffness coefficients. The strain-displacement relationships are now

$$\varepsilon_x = \frac{\partial u}{\partial x} + z\frac{\partial \psi_x}{\partial x}, \quad \varepsilon_y = \frac{\partial v}{\partial y} + z\frac{\partial \psi_y}{\partial y}, \quad \gamma_{xy} = \frac{\partial u}{\partial y} + \frac{\partial v}{\partial x} + z\left(\frac{\partial \psi_x}{\partial y} + \frac{\partial \psi_y}{\partial x}\right),$$

$$\gamma_{yz} = \frac{\partial w}{\partial y} + \psi_y, \quad \gamma_{zx} = \frac{\partial w}{\partial x} + \psi_x. \tag{25}$$

The laminate constitutive equations are obtained through the use of the stress-strain and strain-displacement equations with appropriate integration through the thickness. The form of these equations is assumed here to be

$$\begin{Bmatrix} N_x \\ N_y \\ N_{xy} \\ M_x \\ M_y \\ M_{xy} \\ Q_y \\ Q_x \end{Bmatrix} = \begin{bmatrix} A_{11} & A_{12} & A_{16} & B_{11} & 0 & B_{16} & 0 & 0 \\ A_{12} & A_{22} & A_{26} & 0 & B_{22} & B_{26} & 0 & 0 \\ A_{16} & A_{26} & A_{66} & B_{16} & B_{26} & B_{66} & 0 & 0 \\ B_{11} & 0 & B_{16} & D_{11} & D_{12} & D_{16} & 0 & 0 \\ 0 & B_{22} & B_{26} & D_{12} & D_{22} & D_{26} & 0 & 0 \\ B_{16} & B_{26} & B_{66} & D_{16} & D_{26} & D_{66} & 0 & 0 \\ 0 & 0 & 0 & 0 & 0 & 0 & A_{44} & A_{45} \\ 0 & 0 & 0 & 0 & 0 & 0 & A_{45} & A_{55} \end{bmatrix} \begin{Bmatrix} \partial u/\partial x \\ \partial v/\partial y \\ \partial u/\partial y + \partial v/\partial x \\ \partial \psi_x/\partial x \\ \partial \psi_y/\partial y \\ \partial \psi_x/\partial y + \partial \psi_y/\partial x \\ \partial w/\partial y + \psi_y \\ \partial w/\partial x + \psi_x \end{Bmatrix}$$

or

$$\boldsymbol{F} = \boldsymbol{L}\boldsymbol{e} \tag{26}$$

where, clearly, new definitions of $\boldsymbol{F}$, $\boldsymbol{L}$ and $\boldsymbol{e}$ apply from those given in the first-stage analysis. Here N_x, N_y and N_{xy} are the membrane direct and shear forces per unit length; M_x, M_y and M_{xy} are the bending and twisting moments per unit length; and Q_y and Q_x are through-thickness shear forces per unit length. The laminate stiffness coefficients appearing in $\boldsymbol{L}$ are defined in the usual way as

$$(A_{rs}, B_{rs}, D_{rs}) = \int_{-h/2}^{h/2} Q_{rs}(1, z, z^2)\,dz \quad r, s = 1, 2, 6 \tag{27}$$

and

$$A_{rs} = k_r k_s \int_{-h/2}^{h/2} Q_{rs}\,dz \qquad r, s = 4, 5 \tag{28}$$

wherein the $k_r k_s$ are prescribed shear correction factors. The constitutive relationships of Eq. (26) embrace a range of types of laminate which can correspond to a bifurcational buckling problem, dependant upon the nature of the pre-buckling stress field and the laminate boundary conditions (Leissa 1986, Qatu and Leissa 1993), as mentioned earlier. The B_{12} stiffness coefficient is omitted from $\boldsymbol{L}$ simply because its presence would not be compatible with a plate remaining flat prior to bifurcational buckling taking place. In general, not all the stiffness coefficients appearing in $\boldsymbol{L}$ in Eq. (26) will be present for any one laminate, of course.

The strain energy U of a finite strip in the buckling analysis can be expressed in the same form as given earlier for U_1 in Eq. (9), but now with $\boldsymbol{L}$ and $\boldsymbol{e}$ as given in Eq. (26), of course. The column matrix $\boldsymbol{e}$ can be expressed in the form of Eq. (12) but now with new definitions of $\boldsymbol{d}_i$, as in Eq. (23), and of $\boldsymbol{B}_i$, as recorded in the Appendix. Further, U can be expressed in the form of the right-hand side of Eq. (13) with the typical sub-matrix $\boldsymbol{k}_{ij}$ of the strip stiffness matrix $\boldsymbol{k}$ given again by Eq. (14). In evaluating $\boldsymbol{k}$ direct integration is used in the y-direction and numerical integration in the x-direction, as in the pre-buckling analysis.

The comprehensive expression for the potential energy V_g, of the applied in-plane stresses σ_x^o, σ_y^o and τ_{xy}^o (arising from the first stage of the analysis) acting on the finite strip is (Dawe and Wang 1994, 1995)

$$V_g = \frac{h}{2}\int_{-b/2}^{b/2}\int_O^A \left(\sigma_x^o\left[\left(\frac{\partial u}{\partial x}\right)^2 + \left(\frac{\partial v}{\partial x}\right)^2 + \left(\frac{\partial w}{\partial x}\right)^2\right] + \sigma_y^o\left[\left(\frac{\partial u}{\partial y}\right)^2 + \left(\frac{\partial v}{\partial y}\right)^2 + \left(\frac{\partial w}{\partial y}\right)^2\right]\right.$$
$$+ 2\tau_{xy}^o\left[\frac{\partial u}{\partial x}\frac{\partial u}{\partial y} + \frac{\partial v}{\partial x}\frac{\partial v}{\partial y} + \frac{\partial w}{\partial x}\frac{\partial w}{\partial y}\right] + \frac{h^2}{12}\left\{\sigma_x^o\left[\left(\frac{\partial \psi_x}{\partial x}\right)^2 + \left(\frac{\partial \psi_y}{\partial x}\right)^2\right]\right.$$
$$\left.\left. + \sigma_y^o\left[\left(\frac{\partial \psi_x}{\partial y}\right)^2 + \left(\frac{\partial \psi_y}{\partial y}\right)^2\right] + 2\tau_{xy}^o\left[\frac{\partial \psi_x}{\partial x}\frac{\partial \psi_x}{\partial y} + \frac{\partial \psi_y}{\partial x}\frac{\partial \psi_y}{\partial y}\right]\right\}\right) dxdy. \tag{29}$$

Using the displacement field of Eq. (23) in conjunction with Eq. (29) makes it possible ultimately to express V_g in the form

$$V_g = \frac{1}{2}\boldsymbol{d}^T\boldsymbol{k}_g\boldsymbol{d} \tag{30}$$

where $\boldsymbol{k}_g$ is the strip geometric stiffness matrix of which the typical submatrix $\boldsymbol{k}_{gij}$ ($i, j = 1, 2 \cdots n + 1$) is

$$\boldsymbol{k}_{gij} = h\int_{-b/2}^{b/2}\int_O^A \left[\boldsymbol{G}_{1i}^T\boldsymbol{F}^\circ\boldsymbol{G}_{1j} + \boldsymbol{G}_{2i}^T\boldsymbol{F}^\circ\boldsymbol{G}_{2j} + \boldsymbol{G}_{3i}^T\boldsymbol{F}^\circ\boldsymbol{G}_{3j} + \frac{h^2}{12}(\boldsymbol{G}_{4i}^T\boldsymbol{F}^\circ\boldsymbol{G}_{4j} + \boldsymbol{G}_{5i}^T\boldsymbol{F}^\circ\boldsymbol{G}_{5j})\right] dxdy \tag{31}$$

with

$$\boldsymbol{F}^\circ = \begin{bmatrix} \sigma_x^o & \tau_{xy}^o \\ \tau_{xy}^o & \sigma_y^o \end{bmatrix} \tag{32}$$

and with matrices $\boldsymbol{G}_{1i}$ to $\boldsymbol{G}_{5i}$ defined in the Appendix. Since the pre-buckling stresses have the form of Eq. (22) the strip geometric stiffness matrix can be split into those parts corresponding to the dead stresses and to the live stresses, with the incorporation of a load factor for the live stresses, i.e.,

$$\boldsymbol{k}_g = \boldsymbol{k}_{gD} + \lambda\boldsymbol{k}_{gL}. \tag{33}$$

In evaluating $\boldsymbol{k}_g$, Gaussian numerical integration is used in both the x- and y-directions, typically with five points both across a strip and per spline section along a strip.

The strip total potential energy in the buckling stage is

$$\Pi = U - V_g = \frac{1}{2}\boldsymbol{d}^T\boldsymbol{k}\boldsymbol{d} - \frac{1}{2}\boldsymbol{d}^T(\boldsymbol{k}_{gD} + \lambda\boldsymbol{k}_{gL})\boldsymbol{d}. \tag{34}$$

For the complete plate a similar expression applies in terms of whole-plate matrices $\boldsymbol{K}$, $\boldsymbol{K}_{gD}$, $\boldsymbol{K}_{gL}$ and $\boldsymbol{D}$ which are assembled in the direct stiffness manner and which are assumed to relate to the situation after the kinematic boundary conditions have been applied. On minimising the energy, the set of equations for the eigenvalue problem governing plate buckling becomes

$$(\boldsymbol{K} - \boldsymbol{K}_{gD} - \lambda\boldsymbol{K}_{gL})\boldsymbol{D} = \boldsymbol{0}. \tag{35}$$

Solution for critical values of λ is achieved using the iterative Sturm sequence-bisection procedure and the corresponding eigenvector, representing the buckling mode, is determined through the use of a random force vector.

3. Applications

3.1 General remarks

The developed computer program arising from the analysis described above allows the user the choice of a number of types of spline finite strip model, i.e., models based on the assumption in the displacement field of different degrees, *n*, of crosswise Lagrangian interpolation and different degrees, *k*, of longitudinal spline function. However, in the few applications that are described here, only one type of model is used, corresponding to $n = 3$ and $k = 3$, i.e., cubic interpolation across a strip, with four equi-spaced reference lines, and piecewise-cubic spline representation along a strip (except for ψ_x where such representation is piecewise-quadratic).

The range of boundary conditions that could be accommodated in the developed capability is broad but, for the applications described here, attention is restricted to plates which have the same type of condition on all four edges, and this condition is one of four kinds. For an edge running parallel to the *y*-axis, i.e., at $x = 0$, *A*, the types of kinematic condition applied in the buckling analysis are defined as

S1 condition, $u = v = w = \psi_y = 0$;
S2 condition, $v = w = \psi_y = 0$;
S3 condition, $u = w = \psi_y = 0$;
C1 condition, $u = v = w = \psi_x = \psi_y = 0$;

and conditions on an edge running parallel to the *x*-axis are obtained by replacing *u*, *v*, ψ_x and ψ_y by *v*, *u*, ψ_y and ψ_x, respectively.

The shear correction factors are assumed to have the value 5/6 in the described applications, to be consistent with the presented results of earlier studies based on the use of first-order SDPT.

3.2 Buckling of isotropic plates under pure mechanical and pure thermal loading

Here the two extreme situations of buckling under pure mechanical loading with no temperature effect, and buckling under pure thermal loading with no initial mechanical stress, are considered. The aim is to establish the nature of the convergence properties of the developed FSM in relatively simple situations where comparative solutions are available. The plates considered are square and isotropic, with Poisson's ratio $\nu = 0.3$ and coefficient of thermal expansion $\alpha = 2\times10^{-6}$. In the case of pure mechanical loading the plate is S2 simply supported and subjected to uniform uniaxial stress σ_x^o. Two thickness ratios are considered separately, i.e., $A/h = 10$ and $A/h = 100$. In the case of pure thermal loading, two types of boundary condition on all edges are considered separately, i.e., the S3 simply supported and the C1 clamped conditions. The thickness ratio is then $A/h = 100$.

The FSM results are presented in Table 1 in the form of convergence studies with respect to the number of strips *NS* and the number of spline sections, *q*. Comparative results from several sources are also recorded in Table 1. The buckling coefficient *K* in Table 1 is related to the critical stress $(\sigma_x{}^o)_{cr}$ by the equation $(\sigma_x{}^o)_{cr} = K\pi^2 Eh^2/[12(1-\nu^2)A^2]$. The result of Srinivas and Rao (1969) is an exact solution to the full three-dimensional elasticity equation. The result quoted in Timoshenko and Gere (1961) is exact within the confines of classical plate theory. The results of Gowda and Pandali (1970) correspond to use of the Rayleigh-Ritz method (RRM) in the context of CPT and the results of Thangaratnam and Ramachandran (1989) correspond to use of the FEM using semiloof elements.

Table 1 Buckling of isotropic square plates : convergence of values of K and T_{cr}

Solution method	Buckling coefficient K		Critical temperature T_{cr}	
	A/h = 10	A/h = 100	S3 conditions	C1 conditions
FSM, NS = 8 :				
q = 2	3.737	4.004	63.35	168.52
q = 4	3.732	3.998	63.23	168.07
q = 6	3.731	3.997	63.22	167.55
q = 8	3.731	3.997	63.22	167.47
q = 10	3.731	3.997	63.22	167.45
FSM, q = 8 :				
NS = 2	3.737	4.006	63.35	168.52
NS = 4	3.732	3.998	63.23	167.80
NS = 6	3.731	3.997	63.22	167.52
NS = 8	3.731	3.997	63.22	167.47
NS = 10	3.731	3.997	63.22	167.45
Exact 3-D (1)	3.741	-	-	-
Exact CPT (2)	4.000	4.000	-	-
RRM CPT (3)	-	-	63.27	168.71
FEM (4)	-	-	63.33	167.70

(1) Srinivas and Rao (1969), (2) Timoshenko and Gere (1961), (3) Gowda and Pandalai (1970), (4) Thangaratnam and Ramachandran (1989).

From Table 1 it is clear that the FSM results converge very rapidly with respect to both q and NS, particularly for simply supported plates. The FSM results compare closely with the existing comparative solutions except, as expected, that the CPT result for K for the plate with $A/h = 10$ is significantly higher than both the SDPT FSM and three-dimensional elasticity results due to the neglect of through-thickness shearing effects.

3.3 Thermomechanical buckling of 16-layer, symmetric laminates

Noor and Peters (1992) have considered the thermomechanical buckling of symmetrically-laminated rectangular plates. In their work the plates in general are subjected to a uniform uniaxial stress and a uniform temperature rise. A mixed finite element formulation is used in the context of first-order SDPT : the fundamental unknowns consist of generalized displacements and stress resultants, each of which is represented with bi-quadratic Langrangian shape functions. An efficient multiple-parameter reduction method is used in conjunction with the FEM models. In the presented examples the plates considered are square, with side length 254 mm, and with S2 simple support conditions. The individual plies have a thickness of 0.127 mm and properties, with relation to fibre axes 1 (along) and 2 (across), defined as

E_1 = 130.3 GPa, E_2 = 9.377 GPa, $G_{12} = G_{13}$ = 4.502 GPa,
G_{23} = 1.724 GPa, ν_{12} = 0.33, $\alpha_1 = 0.139\times10^{-6}/^{o}$C, $\alpha_2 = 9.0\times10^{-6}/^{o}$C

Amongst the examples considered are those which concern a 16-layer angle-ply plate of $[\pm45]_{4,S}$ construction and a 16-layer quasi-isotropic plate of $[\pm45/0/90]_{2,S}$ construction. These constructions, each of total thickness h = 2.032 mm, are the ones considered here.

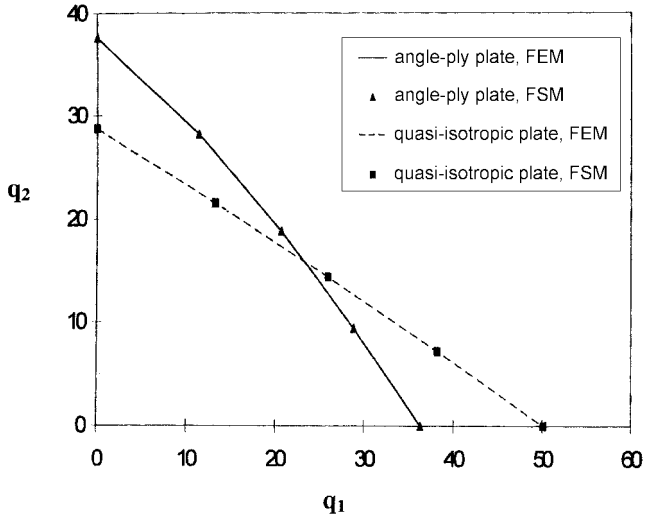

Fig. 3 Stability boundary of 16-layer quasi-isotropic and angle-ply laminates under combined thermal and mechanical loading.

Table 2 Buckling of 16-layer, square plates under combined loading : critical values of q_1 and q_2

$\frac{N_x^o}{(N_x^o)_{cr}}$	Solution method	Quasi-isotropic plates		Angle-ply plates	
		Mode 1	Mode 2	Mode 1	Mode 2
		Pure axial compression : values of q_2			
1.0	FSM	28.71	36.83	37.63	37.66
1.0	FEM*	28.74	36.92	37.64	37.69
		Pure temperature rise: values of q_1			
0	FSM	50.07	104.4	36.26	71.97
0	FEM*	50.13	104.7	36.28	71.92
		Combined loading : values of q_1			
0.75	FSM	13.20	49.96	11.35	21.28
0.75	FEM*	13.21	50.16	11.37	21.36
0.5	FSM	25.90	72.25	20.64	40.75
0.5	FEM *	25.92	72.46	20.66	40.82
0.25	FSM	38.17	93.20	28.82	58.54
0.25	FEM *	38.22	93.42	28.84	58.60

*Noor and Peters (1992)

The FEM results of Noor and Peters are presented in terms of two parameters which are defined as

$$q_1 = \alpha_2 T_o A^2/h^2,\ q_2 = N_x^\circ A^2/E_2 h^3$$

where T_o is the uniform temperature rise and $N_x^o = h\sigma_x^o$ is the uniform axial compressive stress resultant. For particular combinations of q_1 and q_2 an instability will occur. Noor and Peters (1992) present the stability boundary in $q_1 - q_2$ space which separates areas of stability and instability. This is reproduced here in Fig. 3 for the 16-layer angle-ply and quasi-isotropic plates: the stable region for each plate is the region beneath the appropriate curve, of course. On the same figure are shown

the results obtained for these applications when using the present FSM (with $NS = q = 8$). It is clear that there is very close comparison between the sets of FSM and FEM results.

Noor and Peters (1992) also calculate the lowest two critical values of q_1 and q_2 for the two plates for a few different values of the ratio $N_x^o/(N_x^o)_{cr}$ where $(N_x^o)_{cr}$ is the buckling stress resultant corresponding to pure axial compression. These numerical results are recorded in Table 2 together with results generated using the present FSM, again with $NS = q = 8$. The FSM results are generally slightly lower than the corresponding FEM results but the comparison is very close, with the greatest difference being approximately 0.4%.

3.4 Thermomechanical buckling of 4-layer, symmetric and anti-symmetric, cross-ply plates

FSM results are presented here which pertain to the mechanical buckling of plates which have an initial thermal stress field due to a uniform temperature change. These results are compared to those of Sai Ram and Sinha (1992) who considered the buckling of various four-layered, graphite-epoxy laminates of different aspect ratios, with both S1 simply supported and C1 clamped edges, using a finite element method. The element used by Sai Ram and Sinha is an eight-node, 40 degree-of-freedom quadrilateral, employing quadratic serendipity shape functions in defining each of the five displacement-type quantities. The properties of this shear-deformable (first-order SDPT) element are evaluated using Gaussian quadrature. The change in material properties at elevated temperatures was considered and Table 3 shows the assumed variation of E_1, E_2 and G_{12} with temperature, as recorded by Sai Ram and Sinha. Other material properties are that

$G_{13} = G_{12}$, $G_{23} = 0.5G_{12}$, $\nu_{12} = 0.3$, $\alpha_1 = -0.3\times10^{-6}$/°K, $\alpha_2 = 28.1\times10^{-6}$/°K.

In all their applications Sai Ram and Sinha use a 4×4 mesh of equal rectangular elements to model an entire plate, and present no evidence of quality of convergence of calculated buckling loads with

Table 3 Elastic moduli E_1, E_2 and G_{12} of a graphite - epoxy lamina at different temperatures

Elastic moduli (GPa)	Temperature, °K					
	300	325	350	375	400	425
E_1	130	130	130	130	130	130
E_2	9.5	8.5	8.0	7.5	7.0	6.75
G_{12}	6.0	6.0	5.5	5.0	4.75	4.5

Table 4 Buckling of four-layer, cross-ply square plate at 325°K : critical values of λ

Solution method	λ	Solution method	λ
FSM, $NS = 8$:		FSM, $q = 8$:	
$q = 2$	0.4536	$NS = 2$	0.4467
$q = 4$	0.4467	$NS = 4$	0.4467
$q = 6$	0.4467	$NS = 6$	0.4467
$q = 8$	0.4467	$NS = 8$	0.4467
FEM *	0.4488	FEM *	0.4488
RRM *	0.4477	RRM *	0.4477

*Sai Ram and Sinha (1992)

increase in the number of elements used. As a precursor to their presentation of results they have made comparison with a result which they calculated using a Rayleigh-Ritz method of Whitney and Ashton (1971). This comparison is for the buckling under uniform uniaxial compressive stress σ_x^o of a S1 simply supported, square, 0/90/90/0 symmetric cross-ply plate which is heated from the base temperature of 300°K up to 325°K, i.e., $T = 25$°K. For this particular case the lamina properties are assumed to be unaffected by temperature. FSM results have been generated using the present approach for this case in convergence studies with varying values of *NS* and *q*. The complete collection of all results is recorded in Table 4 : these results are values of a non-dimensional critical load factor $\lambda = (N_x^o)_{cr} / [(N_x^o)_{cr}]_{T=300K}$ i.e., the ratio of buckling load at the elevated temperature (which in this example is 325°K) to buckling load at 300°K. It can be seen from the table that, for this relatively simple situation in which the buckled mode shape has one half-wave in each co-ordinate direction there is very close agreement between the three sets of results, and that the FSM results demonstrate very fast convergence. In what follows the FSM results have been generated using $NS = q = 8$ (and the FEM results of Sai Ram and Sinha are for a 4 ×4 mesh).

Continuing with square laminates, Sai Ram and Sinha have presented graphical results for the change of λ when the temperature changes from its base of 300°K up to 425°K (or T varies from 0°K to 125°K). Here we study two plates, one of the same 0/90/90/0 symmetric cross-ply construction considered above, and the other of 45/-45/45/-45 anti-symmetric angle-ply construction. In both cases, plates with all edges S1 simply supported and all edges C1 clamped are considered. Figs. 4 and 5 show the comparison between the FEM results copied from Sai Ram and Sinha (1992) (from Figs. 10 and 13 of that reference) and those calculated using the present FSM approach. It can be seen that generally there is close comparison between the two sets of results, although exceptionally for the clamped 0/90/90/0 plate (see Fig. 4a) the comparison is less close, with the λ values predicted by the FEM being significantly greater than those predicted by the FSM.

Finally, some further, tabulated results are available from the work of Sai Ram and Sinha for 0/90/0/90 anti-symmetric cross-ply plates, for aspect ratios, *A*/*B*, of 0.5 and 2.0 and for thickness ratios, *A*/*h*, of 10, 20, 30 and 40. These results relate to values of λ corresponding to a number of prescribed temperature rises *T*. For clamped boundary conditions the FEM results are recorded,

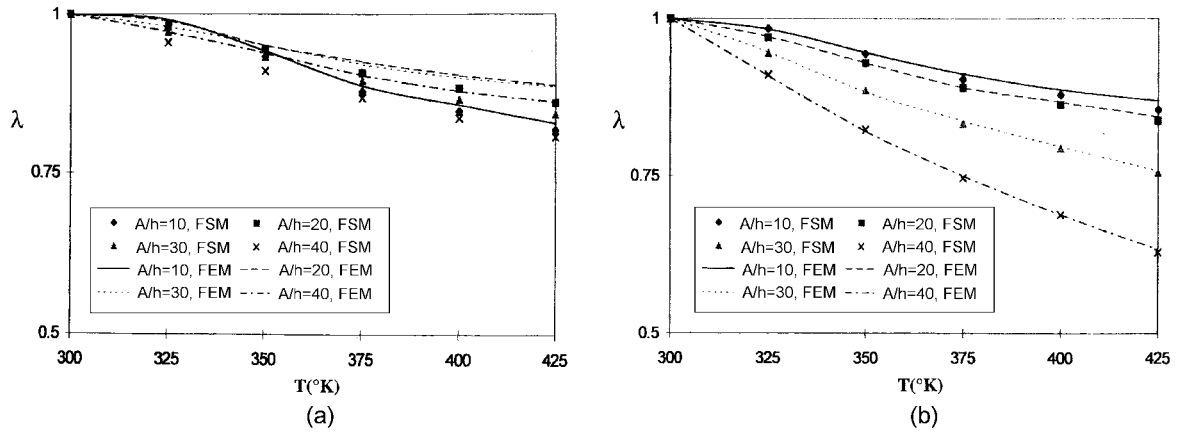

Fig. 4 Effect of temperature on the non-dimensional critical load λ for (0/90/90/0) laminates with (a) clamped C1 boundary, and (b) simply supported S1 boundary.

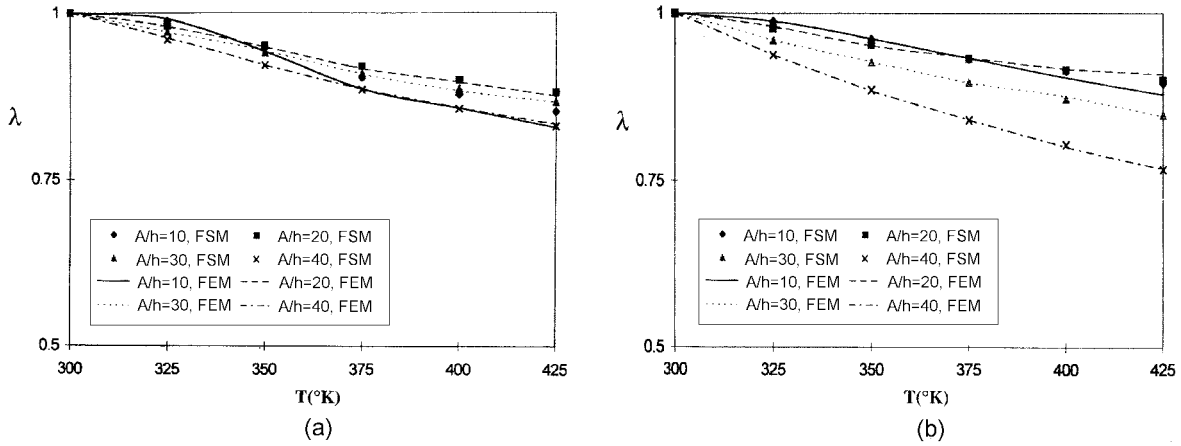

Fig. 5 Effect of temperature on the non-dimensional critical load λ for (45/-45/45/-45) laminates with (a) clamped C1 boundary, and (b) simply supported S1 boundary.

Table 5 Effect of temperature increase T on non-dimensional critical load for 0/90/0/90 clamped rectangular plates

Aspect ratio A/B	Thickness ratio A/h	T = 0°K	T = 25°K	T = 50°K	T = 75°K	T = 100°K	T = 125°K
0.5	10	1.000*	0.985	0.940	0.892	0.864	0.837
		(1.000)*	(0.988)	(0.951)	(0.911)	(0.888)	(0.865)
	20	1.000	0.978	0.945	0.912	0.890	0.870
		(1.000)	(0.980)	(0.954)	(0.928)	(0.909)	(0.893)
	30	1.000	0.967	0.931	0.897	0.872	0.849
		(1.000)	(0.970)	(0.940)	(0.912)	(0.890)	(0.871)
	40	1.000	0.953	0.907	0.865	0.833	0.803
		(1.000)	(0.958)	(0.918)	(0.882)	(0.854)	(0.828)
2.0	10	1.000	0.989	0.922	0.854	0.817	0.781
		(1.000)	(0.994)	(0.931)	(0.865)	(0.828)	(0.792)
	20	1.000	0.981	0.940	0.892	0.864	0.837
		(1.000)	(0.989)	(0.946)	(0.900)	(0.873)	(0.848)
	30	1.000	0.982	0.946	0.909	0.885	0.864
		(1.000)	(0.985)	(0.951)	(0.916)	(0.894)	(0.873)
	40	1.000	0.978	0.945	0.912	0.890	0.870
		(1.000)	(0.982)	(0.951)	(0.919)	(0.898)	(0.880)

*Upper value is FSM result, lower value in parentheses is FEM result (Sai Ram and Sinha 1992)

within parentheses, in Table 5 together with results generated using the present FSM approach. It can be seen from the table that the comparison between the two sets of results is quite close although, at least for the larger values of T_o, not as close as seen earlier for square plates. The greatest difference between any two comparative values is about 3.35%. Perhaps the main reason for the relative lack of closeness is that the 4×4 FEM mesh is insufficiently fine in situations where, as now, the buckling mode shape has more than one half-wave in the direction of the longest plate edge.

4. Conclusions

The scope of the B-spline finite strip method has been extended to allow the prediction of the buckling of rectangular composite laminated plates subjected to combined thermal and mechanical loading. The analysis makes allowance for through-thickness shear effects at the buckling stage and permits consideration of laminates with a range of types of lay-up and of boundary conditions. The method has been applied to the solution of a number of specific problems and has been shown to have good convergence properties to values which generally compare closely with the results of previous studies.

The analysis described herein is of a linear nature, taking place in two distinct stages, namely a pre-buckling stage in which only in-plane behaviour is involved in a perfectly flat configuration (with appropriate restriction on the type of lay-up) and the bifurcational buckling stage wherein out-of-plane displacements develop. The general problem of the full-range response of a plate to thermomechanical loading is nonlinear, of course, but this general problem can also be studied using the B-spline finite strip method, and this will be described in a future publication.

Acknowledgements

The first author gratefully acknowledges the financial support of both the ORS Awards Scheme and The School of Civil Engineering at the University of Birmingham during the period of the investigation reported herein.

References

Chen, L.W., Brunelle, E.J. and Chen, L.Y. (1982), "Thermal buckling of initially stressed thick plates", *J. Mech. Design*, **104**, 557-564.

Cheung, Y.K. and Fan, S.C. (1983), "Static analysis of right box girder bridges by spline finite strip method", *Proc Inst. Civil Engineers*, **75**, 311-323.

Dawe, D.J. and Wang, S. (1992), "Vibration of shear-deformable beams using a spline-function approach", *Int. J. Numer. Methods Eng.*, **33**, 819-844.

Dawe, D.J. and Wang, S. (1994), "Buckling of composite plates and plate structures using the spline finite strip method", *Composites Engineering*, **4**, 1099-1170.

Dawe, D.J. (1995), "Finite strip buckling and postbuckling analysis", In *Buckling and Post-buckling of Composite Plates* (editors Turvey, G.J. and Marshall, I.H.) Chapter 4, 108-153, Chapman & Hall, London.

Dawe, D.J. and Wang, S. (1995), "Spline finite strip analysis of the buckling and vibration of rectangular composite laminated plates", *Int. J. Mech. Sci*., **37**, 645-667.

Dawe, D.J. and Ge, Y.S. (2000), "Thermal buckling of shear-deformable composite laminated plates by the spline finite strip method", *Comput. Methods Appl. Mech. Engrg*, **185**, 347-366.

Gowda, R.M.S. and Pandalai, K.A.V. (1970), "Thermal buckling of orthotropic plates", In *Studies in Structural Mechanics* (editor Pandalai, K.A.V.), 9-44, IIT, Madras.

Leissa, A.W. (1986), "Conditions for laminated plates to remain flat under inplane loading", *Composite Structures*, **6**, 261-270.

Noor, A.K. and Peters, J.M. (1992), "Thermomechanical buckling of multilayered composite plates", *J. Engng Mechanics*, ASCE, **118**, 351-366.

Noor, A.K. and Peters, J.M. (1993), "Thermomechanical buckling and postbuckling of multilayered composite panels", *Composite Structures*, **23**, 233-251.

Qatu, M.S. and Leissa, A.W. (1993), "Buckling or transverse deflections of unsymmetrically laminated plates subjected to in-plane loads", *AIAA Journal*, **31**, 189-194.
Sai Ram, K.S. and Sinha, P.K. (1992), "Hygrothermal effects on the buckling of laminated composite plates", *Composite Structures*, **21**, 233-247.
Srinivas, S. and Rao, A.K. (1969), "Buckling of thick rectangular plates", *AIAA Journal*, **7**, 1645-1646.
Tauchert, T.R. (1995), "Temperature and absorbed moisture", In *Buckling and Post-buckling of Composite Plates*, (editors Turvey, G.J., and Marshall, I.H.) Chapter 5, 190-226, Chapman & Hall, London.
Thangaratnam, K.R. and Ramachandran, J. (1989), "Thermal buckling of composite laminated plates", *Comput. & Structures*, **32**, 1117-1124.
Timoshenko, S.P. and Gere, J.M. (1961), *Theory of Elastic Stability*, 2nd Edition, McGraw-Hill, London.
Turvey, G.J. and Marshall, I.H. (editors) (1995), *Buckling and Post-buckling of Composite Plates*. Chapman & Hall, London.
Wang, S. and Dawe, D.J. (1997), "Spline finite strip analysis of the buckling and vibration of composite prismatic plate structures", *Int. J. Mech. Sci*., **39**, 1161-1180.
Whitney, J.M. and Ashton, J.E. (1971), "Effect of environment on the elastic response of layered composite plates", *AIAA Journal*, **9**, 1708-1713.
Yang, I.H. and Shieh, J.A. (1988), "Generic thermal buckling of initially stressed anti-symmetric cross-ply thick laminates", *Int. J. Solids & Stuctures*, **24**, 1059-1070.

Appendix

Matrices $\boldsymbol{B}_i$ and $\boldsymbol{G}_{1i}$ to $\boldsymbol{G}_{5i}$ of Section 2.3 are defined as

$$\boldsymbol{B}_i = \begin{bmatrix} N_i\overline{\boldsymbol{\Phi}}_k' & \mathbf{0} & \mathbf{0} & \mathbf{0} & \mathbf{0} \\ \mathbf{0} & N_i'\overline{\boldsymbol{\Phi}}_k & \mathbf{0} & \mathbf{0} & \mathbf{0} \\ N_i'\overline{\boldsymbol{\Phi}}_k & N_i\overline{\boldsymbol{\Phi}}_k' & \mathbf{0} & \mathbf{0} & \mathbf{0} \\ \mathbf{0} & \mathbf{0} & \mathbf{0} & \mathbf{0} & N_i\overline{\boldsymbol{\Phi}}_{k-1}' \\ \mathbf{0} & \mathbf{0} & \mathbf{0} & N_i'\overline{\boldsymbol{\Phi}}_k & \mathbf{0} \\ \mathbf{0} & \mathbf{0} & \mathbf{0} & N_i\overline{\boldsymbol{\Phi}}_k' & N_i'\overline{\boldsymbol{\Phi}}_{k-1} \\ \mathbf{0} & \mathbf{0} & N_i'\overline{\boldsymbol{\Phi}}_k & N_i\overline{\boldsymbol{\Phi}}_k & \mathbf{0} \\ \mathbf{0} & \mathbf{0} & N_i\overline{\boldsymbol{\Phi}}_k' & \mathbf{0} & N_i\overline{\boldsymbol{\Phi}}_{k-1} \end{bmatrix}$$

$$\boldsymbol{G}_{1i} = \begin{bmatrix} N_i\overline{\boldsymbol{\Phi}}_k' & \mathbf{0} & \mathbf{0} & \mathbf{0} & \mathbf{0} \\ N_i'\overline{\boldsymbol{\Phi}}_k & \mathbf{0} & \mathbf{0} & \mathbf{0} & \mathbf{0} \end{bmatrix}, \quad \boldsymbol{G}_{2i} = \begin{bmatrix} \mathbf{0} & N_i\overline{\boldsymbol{\Phi}}_k' & \mathbf{0} & \mathbf{0} & \mathbf{0} \\ \mathbf{0} & N_i'\overline{\boldsymbol{\Phi}}_k & \mathbf{0} & \mathbf{0} & \mathbf{0} \end{bmatrix},$$

$$\boldsymbol{G}_{3i} = \begin{bmatrix} \mathbf{0} & \mathbf{0} & N_i\overline{\boldsymbol{\Phi}}_k' & \mathbf{0} & \mathbf{0} \\ \mathbf{0} & \mathbf{0} & N_i'\overline{\boldsymbol{\Phi}}_k & \mathbf{0} & \mathbf{0} \end{bmatrix}, \quad \boldsymbol{G}_{4i} = \begin{bmatrix} \mathbf{0} & \mathbf{0} & \mathbf{0} & N_i\overline{\boldsymbol{\Phi}}_k' & \mathbf{0} \\ \mathbf{0} & \mathbf{0} & \mathbf{0} & N_i'\overline{\boldsymbol{\Phi}}_k & \mathbf{0} \end{bmatrix},$$

$$\boldsymbol{G}_{5i} = \begin{bmatrix} \mathbf{0} & \mathbf{0} & \mathbf{0} & \mathbf{0} & N_i\overline{\boldsymbol{\Phi}}_{k-1}' \\ \mathbf{0} & \mathbf{0} & \mathbf{0} & \mathbf{0} & N_i'\overline{\boldsymbol{\Phi}}_{k-1} \end{bmatrix}$$

where the prime $(\,)'$ denotes differentiation with respect to x for $\overline{\boldsymbol{\Phi}}_k(x)$ and $\overline{\boldsymbol{\Phi}}_{k-1}(x)$ and with respect to y for $N_i(y)$.